Pure and Applied Geophysics

Excitation of Basin-Wide Modes of the Pacific Ocean Following the March 2011 Tohoku Tsunami

MOHAMMAD HEIDARZADEH[1,2] and KENJI SATAKE[2]

Abstract—This study is an attempt towards understanding the sources of long oscillations observed within the Pacific Ocean following the 11 March 2011 Tohoku earthquake. We present evidence that extremely long modes of the Pacific Ocean in the range of 2–48 h were excited by this giant tsunami. A numerical approach was employed to calculate the basin-wide modes of the Pacific Ocean, resulting in 49 modes in the range of 2–48 h. We studied 15 tide-gauge records around the Pacific Ocean in order to extract basin-wide modes of the Pacific Ocean excited by this transoceanic tsunami. Spectral analysis of these tide-gauge records showed that some of the calculated basin-wide modes were indeed excited by the Tohoku tsunami. The observed modes ranged from 2 to 49.8 h. We attributed the long oscillations of the Pacific Ocean during the 2011 Tohoku tsunami to the excitation of these basin-wide modes, which can be grouped into global modes (15–48 h) and regional modes (2–15 h). We classified the signals on the tide gauges into three groups: (1) basin-wide modes (>1.5 h), (2) the tsunami source periods (20–90 min), and (3) local bathymetric effects (<20 min). The average contributions to the total tsunami energy were 6.4 % for the basin-wide mode, 64.1 % for the tsunami source, and 29.5 % for the local bathymetry, although the ratios varied from station to station. Simulations suggest that the amount of contribution of basin effects to the total tsunami energy depends on the location of the tsunami source.

Key words: 11 March 2011 Tohoku earthquake, Pacific Ocean, free oscillation, spectral analysis, basin-wide mode, numerical modeling.

1. Introduction

On 11 March 2011, tsunami waves generated by an *Mw* 9.0 earthquake off the coast of northeast Japan destructively attacked the Pacific coast of Japan and affected almost all other coastlines bordering the Pacific Ocean (Fig. 1). The devastating waves, which ran up as high as about 40 m (MORI *et al.* 2012), caused extensive destruction and a death toll of nearly 20,000 in the near-field along the Pacific coast of Japan (SATAKE *et al.* 2013). With two casualties in the far-field, the March 2011 Tohoku tsunami was the first tsunami to produce far-field fatalities in the Pacific Ocean since the 1964 Alaskan tsunami.

Analysis of sea level records of this giant tsunami showed that it was associated with some unusual phenomena. According to SAITO *et al.* (2013), sea level oscillations induced by this tsunami lasted for about 4–5 days in the Pacific Basin. BORRERO *et al.* (2013) reported that the maximum wave height of this tsunami arrived 30–40 h after the first arrival of tsunami waves in some tide-gauge stations in the Pacific Basin. By using a numerical modeling approach to analyze the 2011 Tohoku tsunami, HEIDARZADEH and SATAKE (2013a) reported several tsunami wave reflections from different coastlines within the Pacific Basin and explained their roles in long-lasting tsunami oscillation.

Given such long-lasting oscillations caused by the March 2011 Tohoku tsunami, the purpose of this research was to study the origins of these long oscillations. In general, several factors may contribute to the extended oscillations of a basin-wide tsunami, among which are: reflections of the tsunami waves from different coasts in the region (e.g., SATAKE *et al.* 1988a), tsunami wave scattering by submarine seamounts (e.g., MOFJELD *et al.* 2001), wave trapping in the shelf region (e.g., RABINOVICH *et al.* 2011; YANUMA *et al.* 1998; VAN DORN 1984), excitation of the basin-wide modes of the Pacific Basin due to the tsunami (e.g., SATAKE *et al.* 1988b; RABINOVICH 2009; HEIDARZADEH *et al.* 2012), and harbor resonance at the location of tide gauges inside harbors (e.g., ZELT *et al.* 1990).

[1] Cluster of Excellence "The Future Ocean", Christian-Albrechts University of Kiel, Otto-Hahn-Platz 1, 24118 Kiel, Germany. E-mail: mheidarzadeh@geomar.de
[2] Earthquake Research Institute (ERI), The University of Tokyo, Tokyo, Japan.

Free oscillation is an important source of long-lasting oscillations and sloshing inside enclosed or semi-enclosed basins. This is typical of harbors and lakes. However, when the source area is large enough, like the one for the March 2011 Tohoku tsunami, it may excite the basin-wide modes of large basins such as the Pacific Basin. An example of this phenomenon is the free oscillations of the Sea of Japan due to the tsunami waves generated by the May 1983 earthquake (*Mw* 7.9). According to SATAKE *et al.* (1988a), this tsunami excited long periods of 208, 104 and 62 min, which were calculated to be the basin-wide modes of the Sea of Japan. CARBAJAL *et al.* (2002) reported resonant oscillations having a dominant period of 36 min inside the Manzanillo Lagoon during the October 1995 Manzanillo tsunami. Resonance oscillations were reported in the Marmara Sea due to the destructive Izmit earthquake and tsunami on August 1999 in this nearly enclosed basin (YALCINER *et al.* 2007). The September 2009 Samoa tsunami caused resonance oscillations that were responsible for localized damage along the Samoan Islands (ROEBER *et al.* 2010).

The Tohoku tsunami of March 2011 presents a unique opportunity to study the basin-wide modes of the Pacific Ocean that can only be excited by such extremely large earthquakes. To examine such a possibility, we first applied a numerical algorithm to estimate the basin-wide modes of the Pacific Basin. We then studied the spectral characteristics of 15 tide-gauge records of the March 2011 Tohoku tsunami (Fig. 1) to examine whether some of the calculated modes of the Pacific Basin are present in the spectra of the observed tide gauge records. A comparative study was performed to determine the contribution of free oscillations of the Pacific Basin to the total energy of the 2011 Tohoku tsunami.
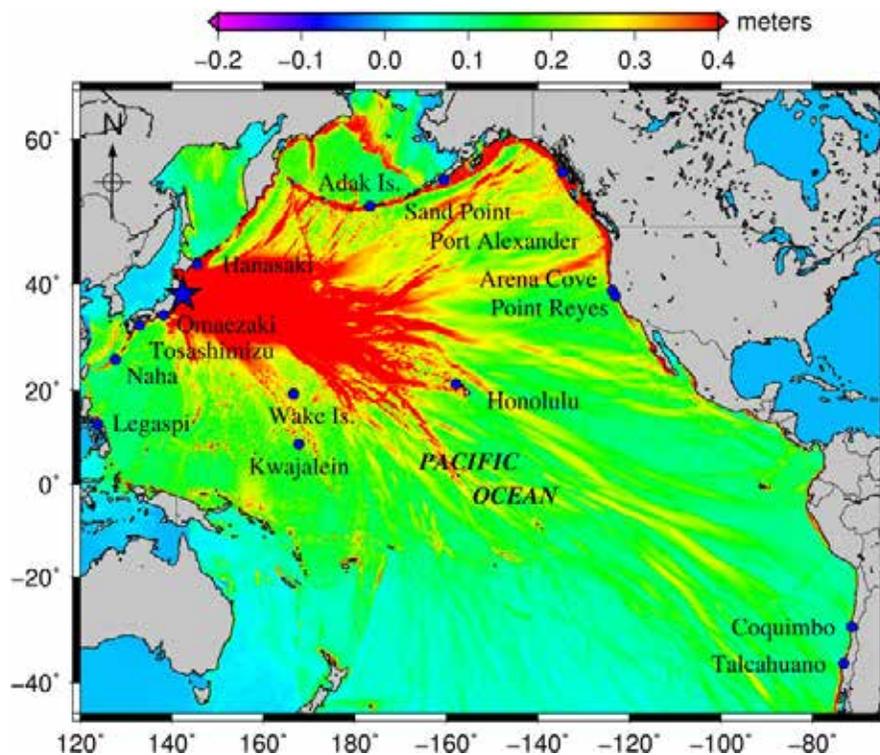

Figure 1
General location map of the Pacific Basin showing the epicenter of the 11 March 2011 *Mw* 9.0 large Tohoku earthquake (*asterisk*) and distribution of the maximum wave height of the resulting tsunami (modified from HEIDARZADEH and SATAKE 2013a). The *solid circles* show the locations of the tide-gauge stations used in this study

2. Calculation of Free Oscillations

The calculation of free oscillations of basins, either enclosed or semi-enclosed, has been studied by numerous ocean scientists using analytical, experimental and numerical methods (e.g., SATAKE et al. 1987; LEE 1971; ZELT et al. 1990; RAICHLEN et al. 1991; YAO 1999; YALCINER et al. 2007). The method used here for calculation of the free oscillation of the Pacific Basin is based on a numerical algorithm proposed by YALCINER et al. (2007), consisting of the following steps:

1. Disturbing the basin with an arbitrary initial wave
2. Simulating the water oscillation using a numerical model
3. Recording time histories of water level oscillations at different locations
4. Calculating spectra of the wave time histories recorded at different locations
5. Free oscillation modes are those periods that are common in most of the spectra

As shown in the following, first we examined the performance of the above algorithm on a rectangular test basin, before applying it to the Pacific Ocean.

2.1. Free Oscillations of a Rectangular Test Basin

The method described above for the calculation of free oscillations of basins was previously tested by YALCINER et al. (2007) for both enclosed and semi-enclosed basins, and was successfully applied to the Marmara Sea in Turkey. Despite this, to show the efficiency of the method, we applied this algorithm to a squared-shaped enclosed basin with a constant water depth of 100 m and a length of 5,000 m. For this test, the basin was disturbed with an initial rectangular crest wave whose length, initial height, and velocity were 300 m, 1 m and 0 m/s, respectively. The conditions of this test case were similar to those of tectonic tsunamis. Snapshots of wave propagation at different times along with spectral analysis for the time histories of waves at selected locations are shown in Fig. 2. A nonlinear, shallow-water numerical code known as TUNAMI was applied for modeling the propagation of the waves (YALCINER et al. 2004). For this test basin, the grid

spacing, simulation time-step and total simulation time were: 20 m, 0.2 s, and 5 h, respectively.

The periods of free oscillations of this test basin can be calculated using the following analytical equation (RABINOVICH 2009):

$$T_{mn} = \frac{2}{\sqrt{m^2 + n^2}} \frac{L}{\sqrt{gd}}, \qquad (1)$$

in which L is the basin's length, g is the gravitational acceleration, d is water depth, m, $n = 0, 1, 2\ldots$ and T_{mn} is the mnth mode. Using this analytical equation, some first modes of free oscillations for this test basin are: 319.3, 159.6, 142.8, 112.9, 106.4, 88.6, 79.8, 77.4, 71.4, 63.9, 59.3, and 53.2 s. Based on Fig. 2, the employed numerical approach was successful in reproducing all of the theoretical values. Figure 2 also shows that the results (i.e., spectral peaks) were not sensitive to the location of the numerical gauges, though the level of spectral power varied from one location to another.

2.2. Free Oscillations of the Pacific Basin

Based on the algorithm presented above, the Pacific Basin was agitated by two initial disturbances consisting of a half-spherical source with a maximum initial height of 8 m at the center, and a uniform rectangular crest wave with an initial height of 8 m. These initial waves were placed at two different locations: one at the center (source 1, Fig. 3) and the other at the northwestern corner of the Pacific Ocean in the vicinity of the actual source of the 2011 Tohoku tsunami (source 2, Fig. 3). The second source seems slightly similar to the actual source of the 2011 Tohoku tsunami. A nonlinear, shallow water numerical code, known as TUNAMI, was applied for modeling the propagation of the generated waves across the Pacific Ocean (YALCINER et al. 2004). An 8-min bathymetric grid extrapolated from the 1-min GEBCO digital atlas (IOC et al. 2003) was used, resulting in a grid of around 15 km × 15 km. The time-step for the numerical modeling was 10 s and simulations were conducted for a total time of 10 days for each case.

Figure 3 presents snapshots of wave simulations at different times. Time histories of sea level oscillations were recorded at 30 numerical wave
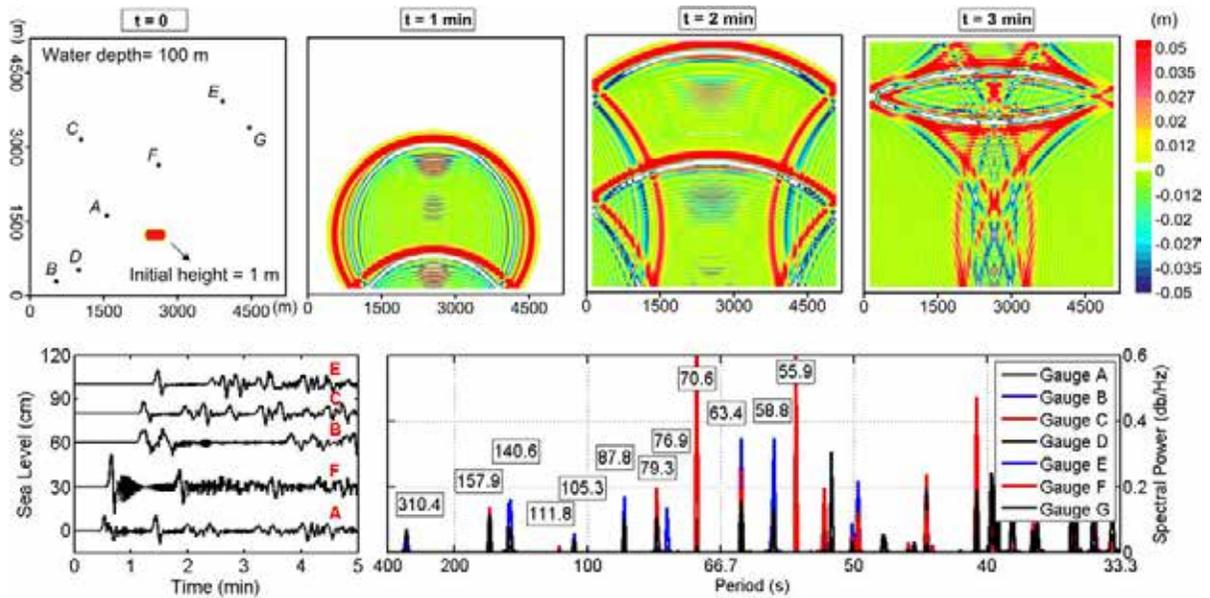
Figure 2
Top snapshots of wave propagation at different times in a square-shaped, enclosed basin with a constant water depth of 100 m, excited by an initial rectangular crest wave with an initial height of 1 m. *Bottom* time histories of wave oscillations and spectral analysis of wave time histories at selected numerical gauges. The locations of the numerical gauges A–G are shown in the *top panel*

gauges. Numerical gauges 1–15 were located at the same locations of the actual tide gauges shown in Fig. 1. The locations of the numerical wave gauges were chosen with the purpose of recording sea level oscillations that were later used for spectral analysis. We show below that this method is not sensitive to the locations of the gauges within the basin.

Results of spectral analysis for these computational sea level records are presented in Fig. 4. The spectra are shown for the periods larger than 1.5 h since basin-wide periods are normally long, of the order of several hours. Figure 4 suggests that the basin-wide peak periods were almost similar for both sources, though the amount of spectral power was different for the two sources. For example, Fig. 4 shows that the spectral powers for periods more than 7 h were larger for source 1 compared to those for source 2 (note that the vertical scales are different in Fig. 4a, b). It seems natural that the amount of energy in a particular period is a function of the location of the initial source. For source 1, because the initial disturbance was located in the middle of the basin, it seems to have been more efficient in exciting basin-wide modes. However, it needs to be noted that only the peak periods are important in this method and the

amount of spectral power in a particular peak period is not important. In fact, in this method, we are interested in discovering all of the available oscillation modes for a basin; it does not matter if those modes are strong or weak.

Different parts of the Pacific Basin may have their own natural periods because of the irregular geometrical shape of the Pacific Basin and the presence of many islands, seamounts, and other aerial or submarine barriers within the Pacific Ocean (Fig. 1). For example, the Hawaiian Islands reflect back part of the tsunami waves generated in offshore Japan, and hence an oscillation may be generated between Japan and Hawaii (USA). Such reflections were evidenced by basin-wide simulations of the March 2011 Tohoku tsunami (NOAA 2013). According to HEIDARZADEH and SATAKE (2013a), the waves generated by the March 2011 Tohoku tsunami arrived in Hawaii 7–8 h after the earthquake, indicating a period of around 14–16 h for the oscillations between Japan and Hawaii. With similar reasoning, we may expect a period of around 18–20 h for the oscillations between California (USA) and Japan because the March 2011 tsunami arrived in California 9–10 h after the earthquake. Although this estimation is rather simplistic, it gives some clues
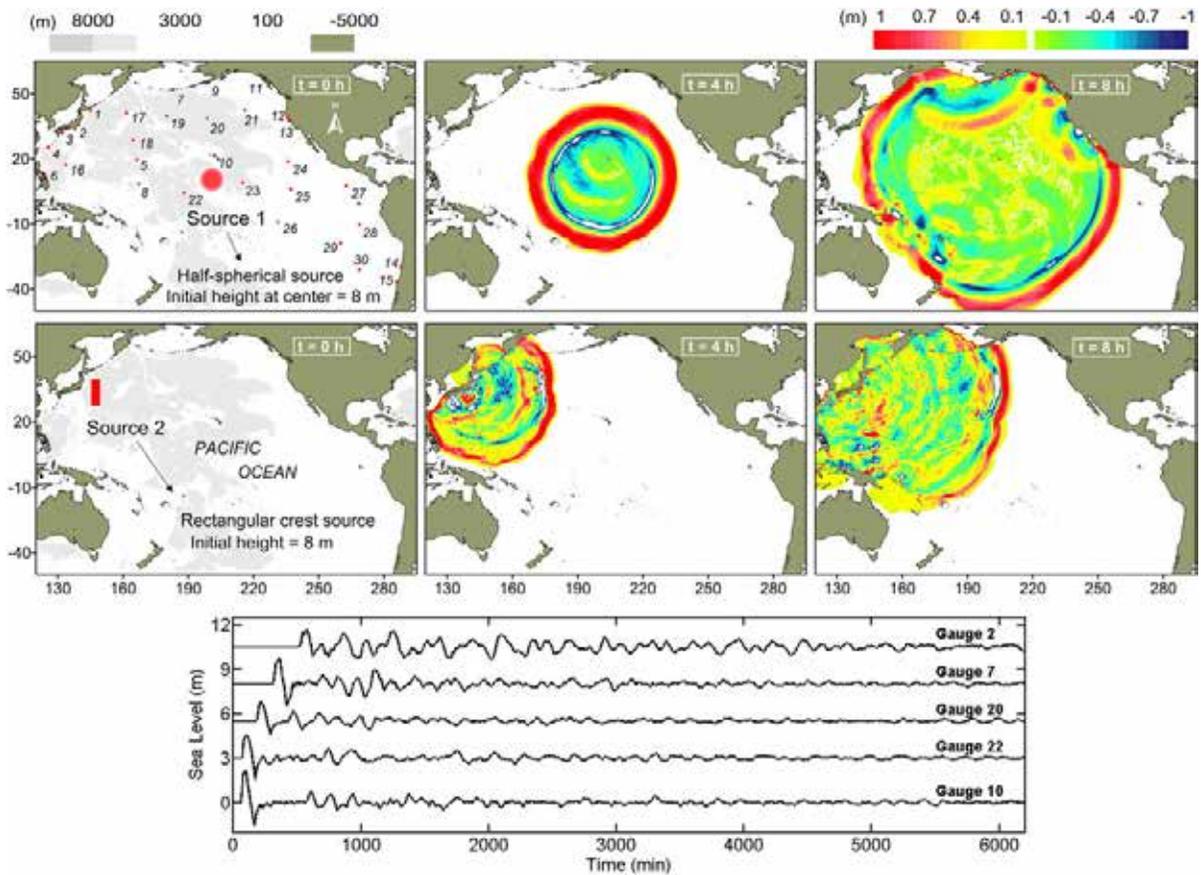
Figure 3
Excitation of the Pacific Basin using a semi-spherical initial source (*top*) and a linear crest initial source (*middle*), and snapshots of the wave evolution at different times. The numbers on the *top–left panel* show the locations of numerical wave gauges. *Bottom* time histories of wave oscillations at selected numerical wave gauges due to source 1

about the order of the modes expected from such a large basin. It is clear that we may expect several modes for the entire Pacific Ocean.

Based on the spectra presented in Fig. 4 for two different sources at 30 different locations, the most common spectral peaks can be considered as the basin-wide modes of the Pacific Ocean. In total, we found 49 basin-wide modes for the entire Pacific Basin, ranging between 2 and 48 h. These modes are: 48.0, 40.0, 34.0, 30.0, 26.7, 24.0, 21.8, 20.0, 15.0, 16.0, 14.1, 13.3, 12.6, 10.9, 10.4, 9.6, 9.2, 8.9, 8.0, 7.7, 7.5, 6.9, 6.7, 6.3, 6.0, 5.9, 5.7, 5.5, 5.3, 5.2, 4.9, 4.4, 4.1, 3.9, 3.8, 3.5, 3.4, 3.3, 3.2, 3.1, 3.0, 2.9, 2.8, 2.7, 2.6, 2.5, 2.4, 2.3, 2.2, 2.1, and 2.0 h. As shown in Fig. 4, the modes above 10 h are relatively weaker than those below 10 h, which seems natural because such long cycles occur only few times during the

whole life of wave oscillations. The longest calculated oscillation mode of the Pacific Ocean is 48 h. Through numerical modeling of the March 2011 Tohoku tsunami, SAITO *et al.* (2013) presented evidence that this extremely long mode was excited during the aforesaid giant tsunami. Figure 4 shows that many spectral peaks are almost the same at different locations, indicating that the results are not influenced significantly by the locations of the numerical gauges. Hence, these locations can be selected arbitrarily.

It seems difficult to precisely determine the origins of each of the basin-wide modes presented above. However, observations from past tsunamis may give us some insights into their origins. In this context, we may classify the basin-wide modes presented above into two groups: regional (2–15 h)
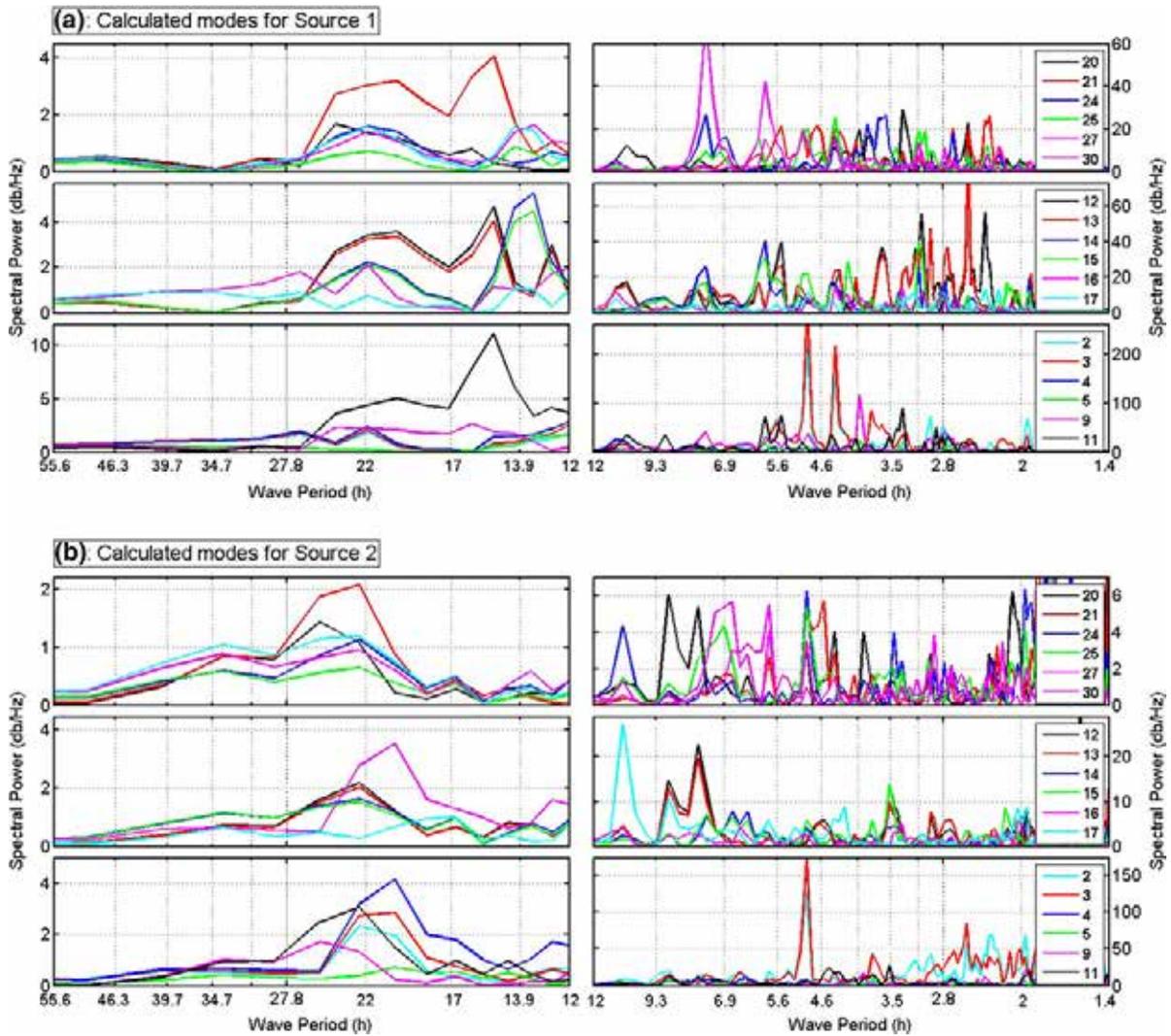
Figure 4
Results of spectral analysis for the wave records of the numerical wave gauges due to a semi-spherical source at the center (**a**) and a linear crest source at the northwest corner of the Pacific Ocean (**b**). Note that the *vertical scales* are different between (**a**) and (**b**)

and global modes (15–48 h). Regional modes are those that belong to different parts of the Pacific Basin, such as the region between Japan and Hawaii, as discussed earlier. Regional modes may have oscillation periods of around 7–15 h. Some other modes in this category with periods in the range of 2–7 h seem not to be the results of reflections from the coasts. These modes are likely the results of wave scattering and reflection from submarine seamounts and other bathymetric features (e.g., wave trapping in shelves). Intensive interactions of tsunami waves with ocean bathymetry are evidenced by basin-wide

simulations of the 2011 Tohoku and 2004 Sumatra tsunamis, suggesting that part of the waves are reflected back and scattered by submarine features before reaching the coastal areas. This is because of the nature of tsunamis, which is a series of long waves having significant interactions with the ocean bottom. Global modes are those belonging to the whole Pacific Basin and are the results of shore-to-shore oscillations. For example, the periods of 21.8 and 24.0 h are among the global modes that likely belong to the oscillations between the West Coast of the US and Japan. As another example, the modes in

the range of 40–48 h are likely to represent the oscillations between the Japanese and South American coasts because the tsunami waves of the March 2011 Tohoku tsunami arrived in Peru and Chile 21–24 h after generation (HEIDARZADEH and SATAKE 2013a).

3. Analysis of the Observed Sea Level Data during the 2011 Tohoku Tsunami

3.1. Methodology

The methodology used here was based on the spectral analysis of the observed sea level records of the March 2011 Tohoku tsunami in order to extract the existing signals and to examine whether or not these signals are the basin-wide modes of the Pacific Basin. To remove the effects of astronomical tides from the sea level spectra, the sea level records were carefully de-tided before spectral analysis. In summary, our methodology consisted of the following steps, which will be briefly explained later:

1. Preparation of the sea level records of the March 2011 Tohoku tsunami,
2. Removing the tidal signal,
3. Spectral analysis of the de-tided signals,
4. Calculating the spectral ratio (tsunami spectra/background spectra), and
5. Identifying basin-wide modes as those modes showing peaks in both spectral plots and spectral-ratio plots

The tide-gauge data used in this study were part of the data previously reported by HEIDARZADEH and SATAKE (2013a). The sea level data were provided through the National Oceanographic and Atmospheric Administration (NOAA, USA), and the UNESCO Intergovernmental Oceanographic Commission (IOC). The locations of these stations are shown in Fig. 1. The data are all of digital type and were sampled at time intervals of 1 min.

In their analysis of the sea level oscillations caused by the March 2011 Tohoku tsunami, HEIDARZADEH and SATAKE (2013a) simply filtered all of the signals having periods larger than 4–5 h from the sea level records. This practice is reasonable because their study was aimed at the detection of the tsunami source periods, which are normally <2 h. However,

the purpose of our study was to detect the basin-wide modes of the Pacific Basin that were possibly excited by the 2011 Tohoku tsunami. These modes are of the order of a few hours to 10 h and greater for a large basin like the Pacific Ocean. Therefore, all of the basin-wide modes could be removed from the sea level records by simple filtering. A band-pass filtering of the data would have been suitable, however, we chose a potentially more appropriate method of precisely calculating the tide using a sophisticated software, and then removing the tidal signal from the original records.

For predicting tidal signal, the tidal analysis package TASK (Tidal Analysis Software Kit, developed at the Proudman Oceanographic Laboratory, UK) was used (BELL et al. 2000). TASK, which has been widely used around the world for tidal analysis, is a collection of Fortran procedures providing full harmonic analysis of the observed tide-gauge data (HEIDARZADEH and SATAKE 2013b). In our tidal analysis, we used 55 major harmonic constituents in order to provide an accurate tidal prediction. The length of the tide-gauge data was 15 days, which means around 21,600 data points, taking into account a sampling interval of 1 min. Fast Fourier Transform (FFT) was used for spectral analysis in this study, for which the Matlab function FFT was applied (MATHWORKS 2013).

3.2. De-tiding of the Observed Signals

Figure 5 presents the de-tided signals of the March 2011 Tohoku tsunami for 15 tide-gauge records from across the Pacific Ocean. For all of the signals, the tide signal was precisely computed using the TASK software and then subtracted from the original signal. Based on Fig. 5, it can be seen that the tidal prediction was precise enough and was able to appropriately remove the tidal effects from the sea level records.

3.3. Averaged Root-Mean-Square (ARMS) of the Data

Different numbers have been reported for the duration of the March 2011 Tohoku tsunami within the Pacific Ocean, ranging from 3 to 6 days (e.g., SAITO et al. 2013; HEIDARZADEH and SATAKE 2013a;
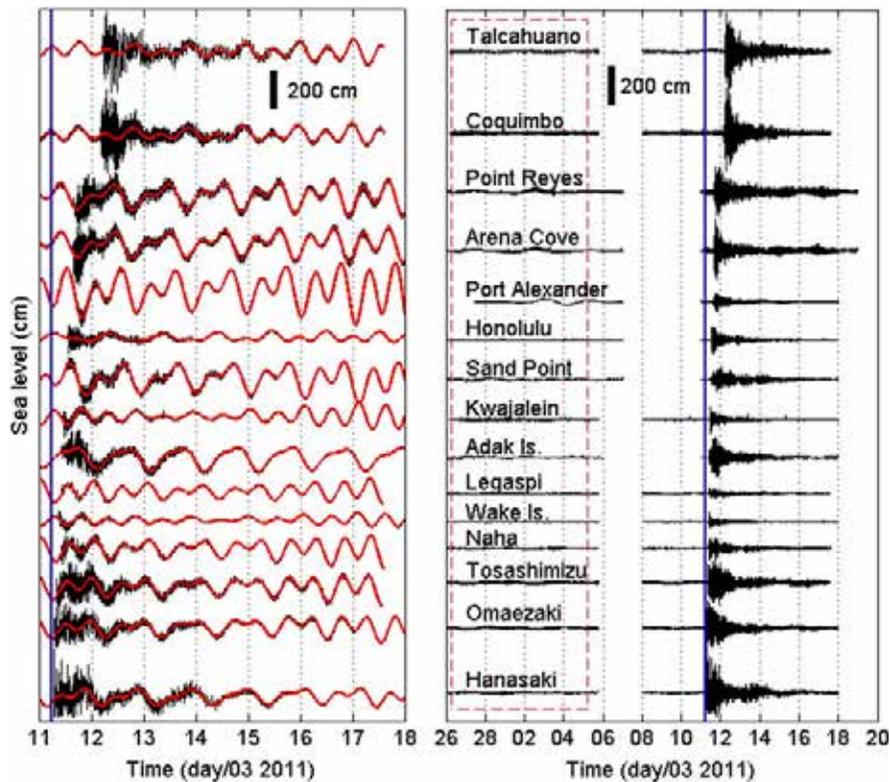
Figure 5
Left observed tide-gauge records of the March 2011 Tohoku tsunami along with the computed tidal signal (the *thick-red lines*). The locations of the tide-gauge stations are shown in Fig. 1. *Right* the de-tided tsunami records after subtracting the computed tidal signal from the original observed tide-gauge records. The *blue vertical line* represents the time of the earthquake occurrence. The *dashed-rectangle* shows the background part of the sea level data used for the calculation of the spectral ratio (color figure online)

BORRERO *et al.* 2013). These estimations were made using a visual look at the filtered tide-gauge records. However, to have a relatively more accurate estimation of the tsunami duration, we calculated the averaged root-mean-square (ARMS) for the 15 de-tided tsunami signals used in this study (Fig. 6a). We defined tsunami duration as the time interval between tsunami arrival (point A, Fig. 6a) and the time that sea level oscillations reached the level of oscillations before the tsunami arrival (point B, Fig. 6a). The results are shown in Fig. 6b, suggesting that the average duration of the tsunami waves was 4.9 days for the 15 tide-gauge records examined.

3.4. Observed Basin-wide Modes of the Pacific during the March 2011 Tsunami

Spectral analysis was performed on the 15 de-tided records of the March 2011 Tohoku tsunami

(Fig. 7a). Based on HEIDARZADEH and SATAKE (2013a), the source periods of this tsunami were in the range of 20–90 min. Figure 7a demonstrates that the signals originating from the tsunami source were the most powerful signals in all of the spectra. An exception is the spectrum for the Port Alexander station, in which the signal with the period of 38.5 h was more powerful than the tsunami source signals. However, it will be shown later that the signal at 38.5 h in Port Alexander was not associated with the tsunami and was possibly a background signal. It can be seen in Fig. 7a that a wide range of signals are available in the sea level spectra; from short-period waves of some minutes to waves with periods of some 10 h.

To examine whether the spectral peaks shown in Fig. 7a were tsunami-related signals or not, we calculated the spectral ratios (tsunami spectra/background spectra) for all of the stations (Fig. 7b). The concept behind spectral ratio (RABINOVICH 1997) is
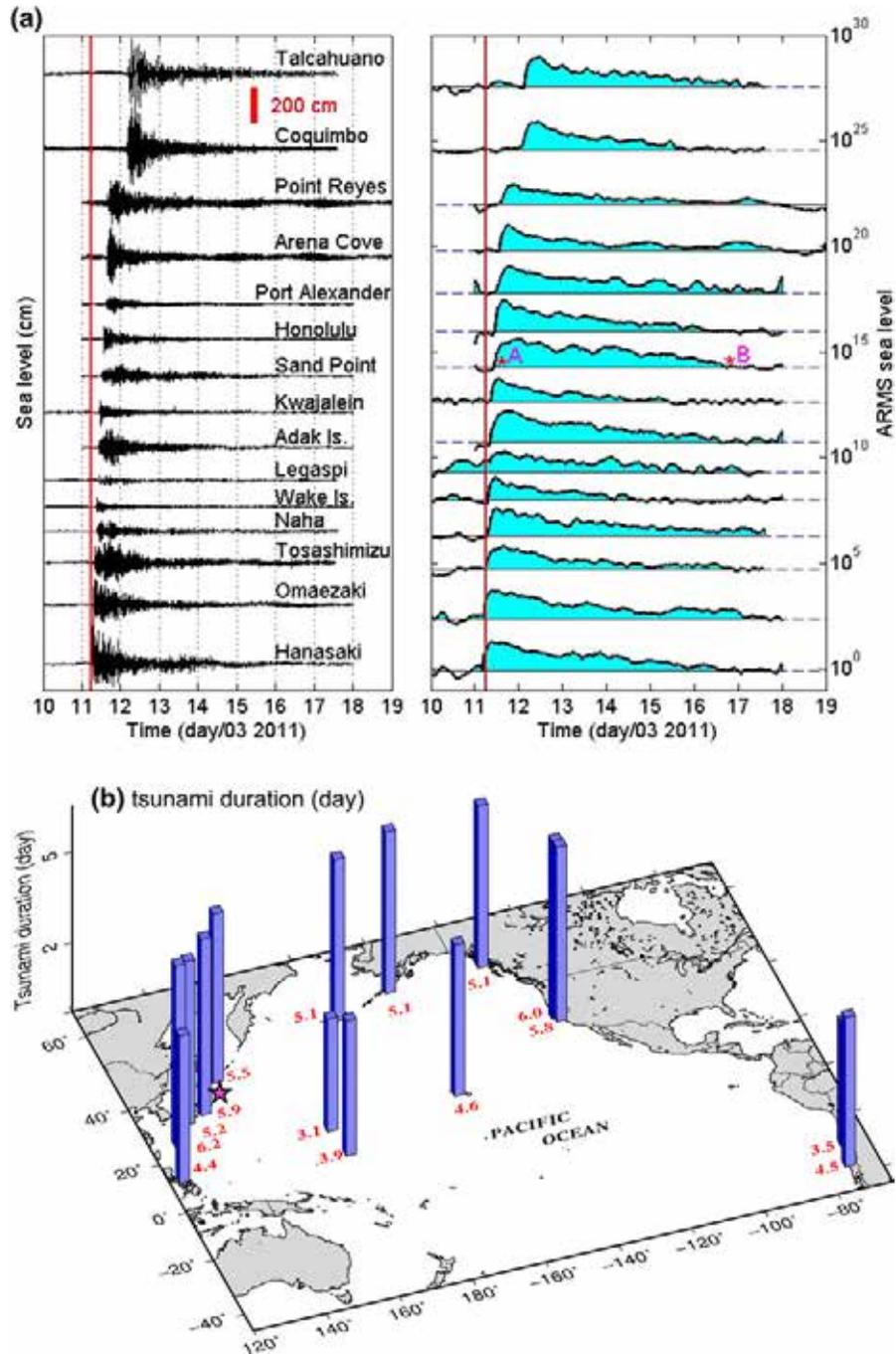
Figure 6
a, *Left panel* de-tided sea level oscillations of the March 2011 Tohoku tsunami, recorded at several tide-gauge stations in the Pacific. **a**, *Rght panel* the respective Averaged-Root-Mean-Square (ARMS) diagrams. The *red line* represents the earthquake time. The *blue-dashed lines* help to calculate tsunami duration. **b** Geographical distribution of the tsunami duration values across the Pacific Ocean (color figure online)

straightforward: if a signal was present in the basin before the tsunami occurrence, the spectral ratio does not show any peak at that frequency because that

signal is counteracted by a similar signal existing in the tsunami waveform. Spectral ratio is free from any local, regional, or global bathymetric effects, and thus
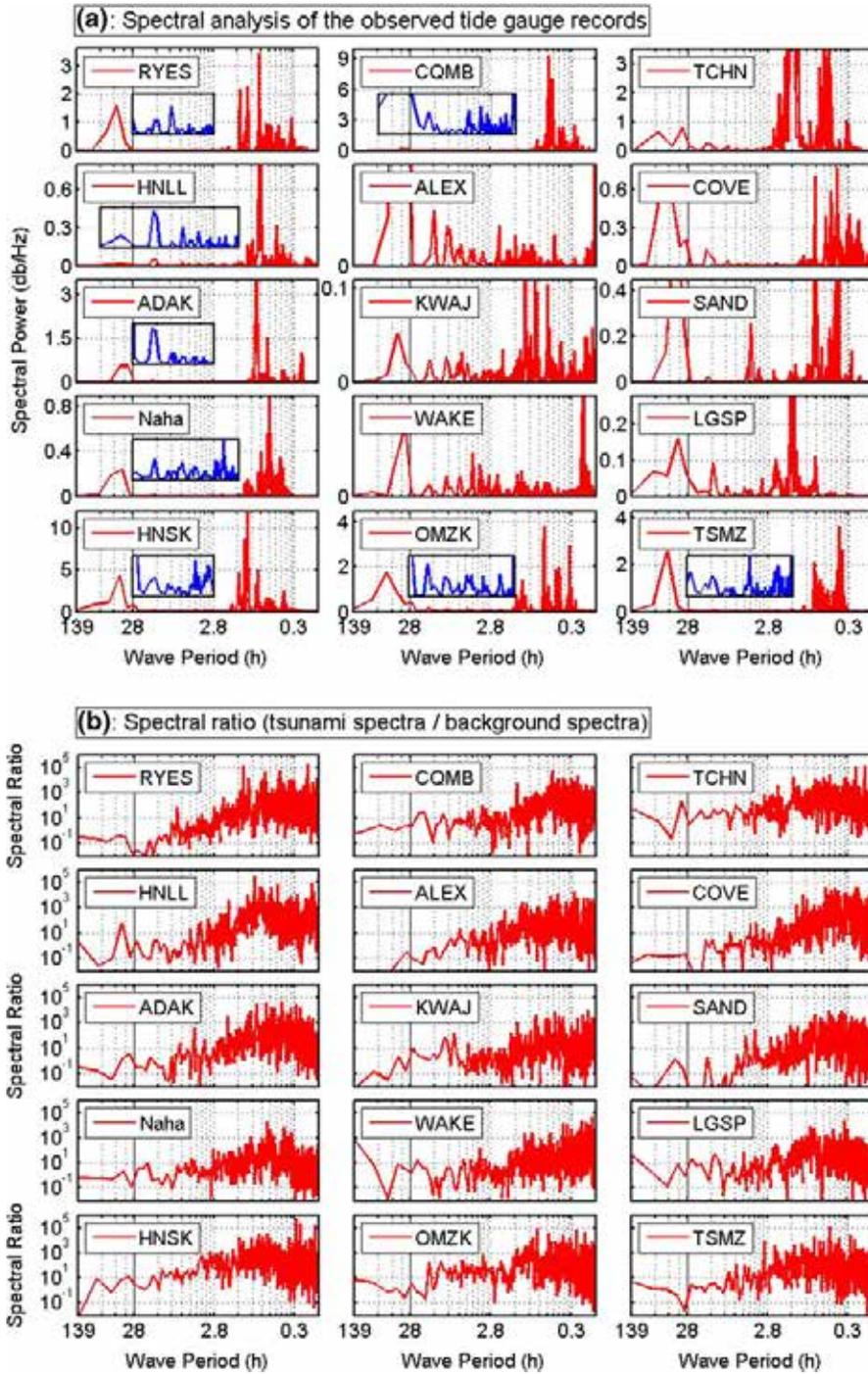
Figure 7

a Results of spectral analysis for actual observed tide-gauge records of the March 2011 Tohoku tsunami. The *insets* show part of the spectra with a better vertical resolution. **b** Spectral ratio (tsunami spectra/background spectra) for the tide-gauge records of the March 2011 Tohoku tsunami. *HNSK* Hanasaki, *OMZK* Omaezaki, *TSMZ* Tosashimizu, *WAKE* Wake Island, *LGSP* Legaspi, *ADAK* Adak Island, *KWAJ* Kwajalein, *SAND* Sand Point, *HMLL* Honolulu, *ALEX* Port Alexander, *COVE* Arena Cove, *RYES* Point Reyes, *CQMB* Coquimbo, *TCHN* Talcahuano

Basin-Wide Oscillations of the Pacific Following the 2011 Tohoku Tsunami

Table 1

Spectral peak periods of the tide-gauge records of the March 2011 Tohoku tsunami. The locations of the tide gauges are shown in Fig. 1. The periods are in hours

Tide-gauge stations

	HNSK	OMZK	TSMZ	Naha	WAKE	LGSP	ADAK	KWAJ	SAND	HNLL	ALEX	COVE	RYES	CQMB	TCHN
Peak periods (h)	2.1	2.1	2.1	2.1	2.1	2.1	2.1	2.1	2.1	2.1	2.1	2.1	2.1	2.1	2.1
	2.3	2.3	2.2	2.5	2.3	2.2	2.3	2.4	2.2	2.2	2.2	2.2	2.3	2.2	2.2
	2.5	2.5	2.3	2.6	2.4	2.3	2.4	2.5	2.4	2.4	2.3	2.5	2.5	2.4	2.3
	2.8	2.7	2.6	2.7	2.5	2.5	2.5	2.7	3.4	2.8	2.4	2.8	2.7	2.5	2.4
	3.1	2.9	2.8	2.9	2.6	2.8	2.7	3.0	3.6	3.1	2.7	2.9	3.0	2.8	2.5
	3.3	3.0	3.0	3.2	2.8	2.9	2.8	3.2	4.6	3.3	3.0	3.0	3.2	3.0	2.7
	3.4	3.2	3.3	3.6	2.9	3.4	3.0	3.3	5.0	3.7	3.1	3.5	3.4	3.2	2.8
	3.6	3.4	3.8	3.8	3.0	4.2	3.2	3.7	6.5	3.9	3.4	3.8	3.7	3.4	2.9
	3.8	3.7	4.3	4.2	3.2	4.6	3.4	4.3	7.1	4.3	3.7	4.5	5.0	3.7	3.2
	4.3	3.8	4.7	4.5	3.5	4.9	3.7	4.6	9.7	5.2	4.2	4.8	5.5	4.7	3.8
	4.6	4.2	5.0	4.8	3.8	5.5	4.6	4.9	15.5	5.5	4.5	5.2	6.8	5.2	4.3
	5.2	4.7	5.3	5.3	4.3	7.4	4.9	5.4	38.9	6.7	5.0	6.5	7.7	6.9	5.2
	5.8	5.4	7.5	6.8	4.7	9.2	6.6	6.3		9.1	5.7	7.4	9.3	8.7	6.8
	6.4	5.8	8.3	8.8	5.0	13.4	7.5	7.1		15.4	6.4	8.8	14.7	10.0	8.6
	7.3	6.2	9.3	10.0	5.5	16.3	8.3	7.8		38.7	7.3	10.4	18.5	13.0	10.0
	9.0	6.7	13.6	14.9	6.6	36.8	9.3	9.8			9.6	16.1	44.0	16.3	16.2
	10.1	7.7	16.6	24.9	8.4		15.8	15.7			14.0			32.6	32.4
	14.7	10.1	24.9	37.4	9.9		31.5	39.3							
	27.0	13.4	49.8		13.2		39.4								
	40.3	16.1			15.9										
		27			31.7										

HNSK Hanasaki, *OMZK* Omaezaki, *TSMZ* Tosashimizu, *WAKE* Wake Island, *LGSP* Legaspi, *ADAK* Adak Island, *KWAJ* Kwajalein, *SAND* Sand Point, *HMLL* Honolulu, *ALEX* Port Alexander, *COVE* Arena Cove, *RYES* Point Reyes, *CQMB* Coquimbo, *TCHN* Talcahuano

is an ideal criterion for identifying tsunami-related signals. The concept of spectral ratio was successfully applied by VICH and MONSERRAT (2009) to the sea level data of the May 2003 tsunami in the western Mediterranean Sea.

We refined the spectra presented in Fig. 7a using the results of the spectral ratios (Fig. 7b). Part of the sea level data used as the background signal is shown with a dashed-rectangle in Fig. 5, and the results of the spectral-ratio calculations are shown in Fig. 7b. For this refinement, we ignore the spectral peaks in Fig. 7a, for which no peaks were available in the spectral-ratio plots (Fig. 7b). In general, most of the observed peaks in the spectra (Fig. 7a) also showed a peak in the spectral-ratio plots (Fig. 7b). However, there were some exceptions. As an example, the large peak at the period of 38.5 h in Port Alexander did not repeat at the spectral-ratio plot for this station, indicating that it was not likely to be associated with the tsunami. As other examples, the peak periods of 64.8 and 58.9 h, observed at the spectra of Talcahuano

and Arena Cove, respectively, do not show any peak at the spectral-ratio plots of these stations and thus were considered as non-tsunami signals.

Table 1 presents all of the signals with periods longer than 2 h available in the tsunami spectra, shown in Fig. 7a after refinement using spectral-ratio plots. We assume that these signals are those that were excited by the 2011 Tohoku tsunami in the Pacific Ocean for two reasons: first, the tidal signals have been carefully removed from the sea level oscillations. Second, other possible non-tsunami signals have been refined from the sea level data using the concept of spectral ratio. Some of these signals were directly excited by the tsunami source (those with periods in the range of 20–90 min), some of them were the results of regional and global oscillations, and others were generated by scattering and reflections from bathymetric features, e.g., wave trappings in shelves and harbor resonance. It can be seen that some of the calculated modes (Sect. 2.2) were observed during the March 2011 Tohoku
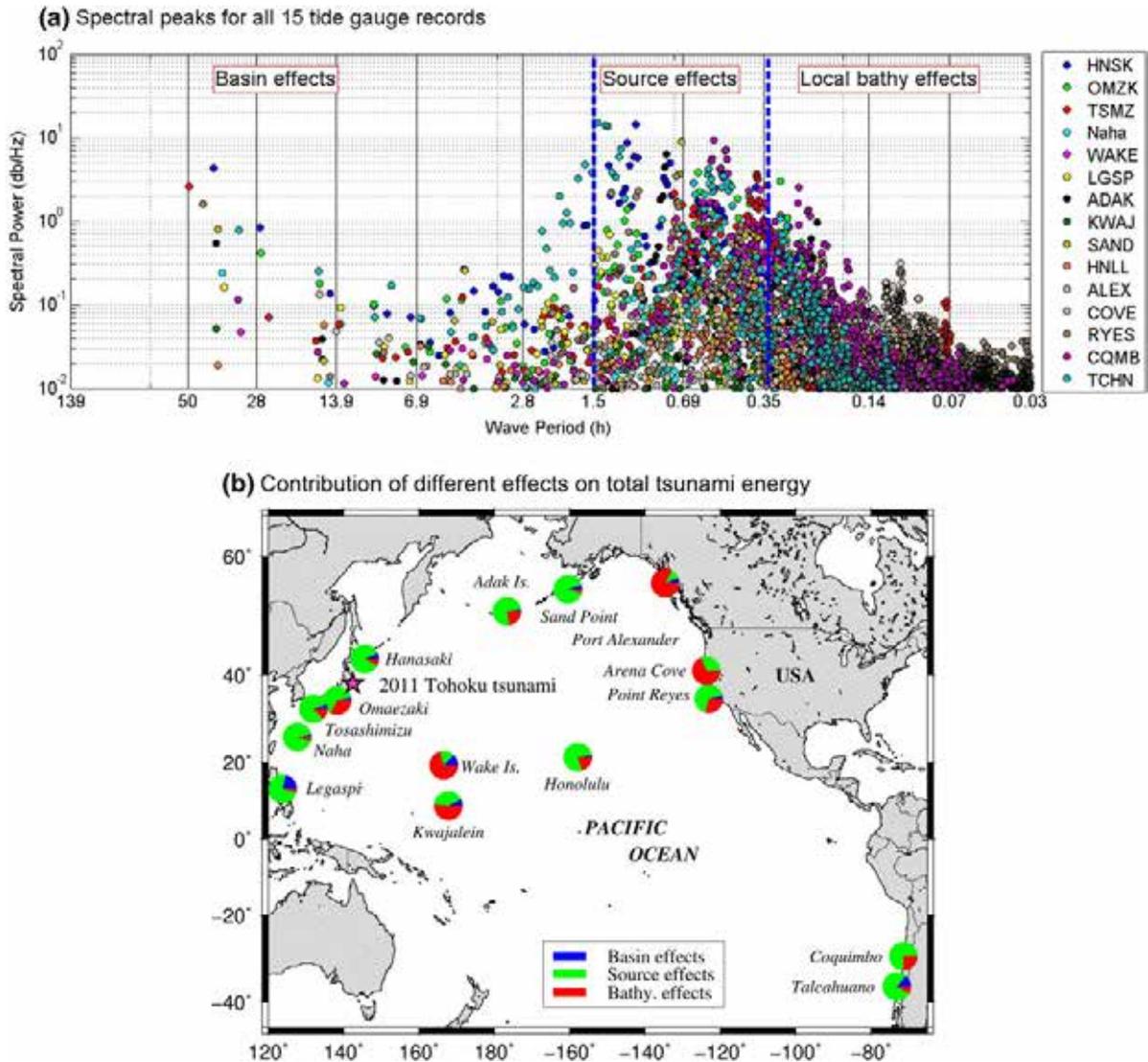
Figure 8

a Spectral peaks for all 15 tide-gauge records of the March 2011 Tohoku tsunami. The *thick-dashed lines* show the border between tsunami energy from local bathymetric effects, tsunami source, and basin effects. **b** Geographical distribution of contribution of different effects on total tsunami energy using *pie graphs*. *HNSK* Hanasaki, *OMZK* Omaezaki, *TSMZ* Tosashimizu, *WAKE* Wake Island, *LGSP* Legaspi, *ADAK* Adak Island, *KWAJ* Kwajalein, *SAND* Sand Point, *HMLL* Honolulu, *ALEX* Port Alexander, *COVE* Arena Cove, *RYES* Point Reyes, *CQMB* Coquimbo, *TCHN* Talcahuano

tsunami (Table 1). Based on Table 1, long modes ranging from 2 to 48 h were excited by the Tohoku tsunami.

4. Discussions

Figure 8a presents the spectral peaks for all 15 tide-gauge records of the March 2011 Tohoku

tsunami. In general, the pattern of tsunami energy distribution over frequency domain is bell-shaped, with its maximum energy occurring at the period dictated by the tectonic source. According to HEI-DARZADEH and SATAKE (2013a), the main tsunami periods of the Tohoku tsunami were 37 and 67 min. Figure 8a shows that the maximum tsunami energy occurred around the period band of 30–70 min and then decreased in both sides.

Although it is difficult to classify different signals observed on a tide gauge into certain groups, we attempted to estimate the contribution of different effects to the total tsunami energy. We classified the spectral peaks shown in Fig. 8a as belonging to one of the three groups: (1) signals generated by basin effects with periods longer than 1.5 h, which include global modes (15–48 h) and regional modes (2–15 h), (2) signals generated by the main tsunami source with periods in the range of 20–90 min, and (3) signals generated by local bathymetric effects with periods shorter than 20 min. As an example, the spectral analysis of sea level records in Wake Island station (Fig. 7a) showed that the peak tsunami energy occurred at the period of around 10 min in this station, indicating that local bathymetric effects such as harbor resonance were responsible for that. In other words, some local modes were excited by the incoming tsunami waves and the amount of energy generated by these local modes through persistent oscillations was higher than that generated by direct tsunami waves.

To calculate the contribution of each of the above effects to the total tsunami energy, we summed the spectral powers for all signals lying in each category. Table 2 presents a summary of the contribution of the three effects to the total energy of the Tohoku tsunami for all 15 tide-gauge records. The geographical distribution of the data is shown in Fig. 8b using pie graphs. According to Table 2 and Fig. 8b, most of the tsunami energy came from its tectonic source, and the contributions by other effects to the total energy were relatively small. On the average, the contributions of basin effects, tsunami source, and local bathymetry to the total tsunami energy were 6.4, 64.1 and 29.5 %, respectively. The contribution of basin effects to the total tsunami energy ranged from 0.4 % in Coquimbo to 21.8 % in Legaspi. In most of the examined tide-gauge records, the contribution of basin effects was smaller than those of tsunami source and local bathymetry, which is expected due to the limited number of cycles passed by such long modes during the whole life of the Tohoku tsunami. For all records, the contribution of basin effects to the total tsunami energy was smaller than that of tsunami source. In three stations of Legaspi, Talcahuano and Sand Point, the contribution of basin effects to the total tsunami energy was larger than that of local effects.

Table 2

Contribution of local bathymetry, tsunami source, and basin effects to the total tsunami energy of the March 2011 Tohoku tsunami

Station name	Amount of energy (db/Hz)			Contribution to tsunami energy (%)		
	Basin effects[a] (db/Hz)	Tsunami[b] source (db/Hz)	Local bathy[c] (db/Hz)	Basin effects (%)	Tsunami source (%)	Local bathy (%)
Hanasaki	9.2	117.2	10.7	6.7	85.5	7.8
Omaezaki	2.1	36.8	18.8	3.7	63.7	32.6
Tosashimizu	3.8	59.5	9.2	5.2	82.1	12.7
Naha	0.4	13.4	0.6	2.8	92.9	4.2
Wake Is.	0.3	0.4	1.5	13.1	16.6	70.3
Legaspi	1.1	3.6	0.2	21.8	74.3	3.9
Adak Is.	0.7	25.4	7.5	2.1	75.6	22.3
Kwajalein	0.4	2.3	2.8	7.4	41.3	51.3
Sand Point	1.4	24.6	1.1	5.2	90.8	4.1
Honolulu	0.3	9.9	2.5	2.3	78.1	19.6
Port Alexander	0.3	0.5	4.0	6.5	10.7	82.8
Arena Cove	0.4	13.1	30.1	0.9	30.1	69.0
Point Reyes	2.3	37.2	16.2	4.2	66.7	29.0
Coquimbo	0.5	98.1	33.1	0.4	74.5	25.2
Talcahuano	21.3	120.1	12.8	13.8	77.9	8.3
Average	3.0	37.5	10.1	6.4	64.1	29.5

[a] Signals with periods longer than 1.5 h

[b] Signals with periods between 1.5 h and 20 min

[c] Signals with periods shorter than 20 min

Table 2 gives useful information about the complex behavior of tsunami waves in large basins. Out of the 15 tide-gauge records studied here, the contributions of local bathymetry to the total tsunami energy were the largest in the four stations of Wake Island, Kwajalein, Port Alexander, and Arena Cove (Table 2; Fig. 8b). For Wake Island, Table 2 shows that 70.3 % of the total tsunami energy was generated by local bathymetric effects, while direct tsunami waves and basin effects contributed 16.6 and 13.1 % to the total tsunami energy, respectively. As briefly discussed above, significant energy in the period band of 0–20 min can be attributed to the resonance of the harbor in which the tide gauge is located or other bathymetric features like wave focusing and refracting in coastal areas. However, harbor resonance and other coastal bathymetric effects due to incident tsunami waves are not new and were evidenced during some past tsunamis. Long-lasting oscillations in Port Salalah, Oman, were reported following the 2004 Indian Ocean tsunami (OKAL et al. 2006). Our study shows that the energy generated by local bathymetric effects was larger than that generated by direct tsunami waves in 4/15 studied stations.

The results of wave simulations for two different sources, one at the center of the Pacific Ocean and the other at a corner (Fig. 3), show that the strength of basin-wide modes possibly depends on the location of the source. The spectral powers calculated for 30 locations within the Pacific Ocean for two different sources show that the spectral powers are noticeably larger for the source located at the center of the Pacific Ocean (Fig. 4a) compared to the other source (Fig. 4b). In other words, the contribution of basin effects to the total tsunami energy, which was 6.4 % for the March 2011 Tohoku tsunami, may be different for large Pacific tsunamis occurring in different tsunamigenic locations within the Pacific Ocean.

5. Conclusions

To understand the origins of long Pacific Ocean oscillations during the March 2011 Tohoku tsunami, we calculated basin-wide modes of the Pacific Basin using a numerical approach and then studied 15 tide-gauge records of this tsunami to examine which

modes were excited by this giant tsunami. Our main findings were:

1. Using a numerical approach, 49 basin-wide modes were calculated for the Pacific Ocean, ranging from 2 to 48 h.
2. An analysis of 15 tide-gauge records of the March 2011 Tohoku tsunami showed that some of the basin-wide modes of the Pacific Basin were excited by this giant tsunami.
3. To measure the contribution of basin-wide modes to the total tsunami energy, we classified all signals available in a tide-gauge record into three groups: (1) signals generated by basin effects with periods longer than 1.5 h, (2) signals generated by the main tsunami source with periods in the range of 20–90 min, and (3) signals generated by local bathymetric effects with periods shorter than 20 min. On average, the contributions of basin effects, tsunami source, and local bathymetry to the total tsunami energy were 6.4, 64.1, and 29.5 %, respectively.
4. The results of wave simulations for two different sources, one at the center of the Pacific Ocean and the other at a corner, show that the strength of basin-wide modes and their contributions to total tsunami energy possibly depends on the location of the tsunami source.

REFERENCES

BELL, C., VASSIE, J.M., and WOODWORTH, P.L. (2000). POL/PSMSL Tidal Analysis Software Kit 2000 (TASK-2000), Permanent Service for Mean Sea Level. CCMS Proudman Oceanographic Laboratory, UK, 22p.

BORRERO, J.C., and GREER, S.D. (2013). *Comparison of the 2010 Chile and 2010 Japan tsunamis, in the Far-field*, Pure App. Geophys., *170*, 6-8, 1249-1272.

CARBAJAL, N., and GALICIA-PEREZ, M.A. (2002). *Earthquake induced Helmoltz resonance in Manzanillo lagoon, Mexico*. Revista Mexicana de Fisca, *40*, 3, 192–196.

HEIDARZADEH, M., and SATAKE, K. (2012). *Free mode excitation of the Pacific Basin during the 2011 large Tohoku tsunami*. Proceedings of the Japan Geoscience Union Meeting, Paper No. HDS06-P02, 20-25 May 2012, Makuhari, Chiba, Japan.

HEIDARZADEH, M., and SATAKE, K. (2013a). *Waveform and Spectral Analyses of the 2011 Japan Tsunami Records on Tide Gauge and DART Stations Across the Pacific Ocean*. Pure App. Geophys., *170*, 6-8, 1275-1293.

HEIDARZADEH, M., and SATAKE, K. (2013b). *The 21 May 2003 Tsunami in the Western Mediterranean Sea: Statistical and Wavelet Analyses*. Pure App. Geophys., *170* (9-10), 1449-1462.

IOC, IHO, and BODC (2003). *Centenary edition of the GEBCO digital atlas*, published on CD-ROM on behalf of the Intergovernmental Oceanographic Commission and the International Hydrographic Organization as part of the general bathymetric chart of the oceans. British oceanographic data centre, Liverpool.

LEE, J., (1971). *Wave induced oscillations in harbors of arbitrary geometry*. J. Fluid Mechanics, *45*, 375–394.

MATHWORKS (2013). *MATLAB user manual*, The Math Works Inc., MA, USA, 282 p.

MOFJELD, H.O., TITOV, V.V., GONZALEZ, F.I., and NEWMAN, J.C. (2001). *Tsunami scattering provinces in the Pacific Ocean*. Geophys. Res. Lett., *28*, 335–337.

MORI, N., TAKAHASHI, T, and the 2011 Tohoku Earthquake Tsunami Joint Survey Group (2012). *Nationwide Post Event Survey and Analysis of the 2011 Tohoku Earthquake Tsunami*, Coastal Eng. J., *54*, 1, 1-27.

NOAA (2013). *Japan (East Coast of Honshu) Tsunami, March 11, 2011*. Pacific Marine Environmental Laboratory, National Oceanic and Atmospheric Administration. Available at: http://nctr.pmel.noaa.gov/honshu20110311/.

OKAL, E. A., FRITZ, H. M., RAAD, P. E., SYNOLAKIS, C., AL-SHIJBI, Y., and AL-SAIFI, M. (2006). *Oman field survey after the December 2004 Indian Ocean tsunami*. Earthquake Spectra, *22*, S3, 203-218.

RABINOVICH, A.B. (1997). *Spectral analysis of tsunami waves: Separation of source and topography effects*, J. Geophys. Res., *102*, 12, 663–676.

RABINOVICH, A. B., CANDELLA, R. N. and THOMSON, R. E. (2011). *Energy Decay of the 2004 Sumatra Tsunami in the World Ocean*. Pure App. Geophys., *168*, 1919-1950.

RABINOVICH, A.B. (2009). *Seiches and harbor oscillations*, in Handbook of Coastal and Ocean Engineering (edited by Y.C. Kim), Chapter 9, World Scientific Publ., Singapore, 193-236.

RAICHLEN, F., and LEE, J. (1991). *Oscillation of Bays, Harbors, and Lakes*. In: Herbich, J. (Ed.), Handbook of Coastal and Ocean Engineering. Gulf Publishing Co, Houston.

ROEBER, V., YAMAZAKI, Y., and CHEUNG, K.F. (2010). *Resonance and impact of the 2009 Samoa tsunami around Tutuila, American Samoa*. Geophysical Research Letters, 37, L21604, doi:10.1029/2010GL044419.

SAITO, T., INAZU, D., TANAKA, S., and MIYOSHI, T. (2013). *Tsunami Coda across the Pacific Ocean Following the 2011 Tohoku-Oki Earthquake*. Bull. Seismol. Soc. Am., *103*, 2B, 1429-1443.

SATAKE, K., FUJII, Y., HARADA, T., NAMEGAYA, Y. (2013). *Time and space distribution of coseismic slip of the 2011 Tohoku earthquake as inferred from tsunami waveform data*. Bull. Seismol. Soc. Am., *103*, 2B, 1473-1492.

SATAKE, K., and SHIMAZAKI, K. (1987). *Computation of tsunami waveforms by a superposition of normal modes*. J. Phys. Earth, *35*, 5, 409-414.

SATAKE, K., and SHIMAZAKI, K. (1988a). *Free oscillation of the Japan Sea excited by earthquakes-I. Observation and wave-theoretical approach*. Geophys. J. Int., *93*, 3, 451-456.

SATAKE, K., and SHIMAZAKI, K. (1988b). *Free oscillation of the Japan Sea excited by earthquakes- II. Modal approach and synthetic tsunamis*. Geophys. J. Int., *93*, 3, 457-463.

VAN DORN, W. G. (1984). *Some tsunami characteristics deducible from tide records*. J. Phys. Oceanogr., *14*, 2, 353-363.

VICH, M.M., and MONSERRAT, S. (2009). *Source spectrum for the Algerian tsunami of 21 May 2003 estimated from coastal tide gauge data*, Geophys. Res. Lett., 36, L20610.

WESSEL, P. and SMITH, W. H. F. (1991). *Free software helps map and display data*, EOS Trans. AGU 72, 441.

YALCINER, A.C., PELINOVSKY, E., TALIPOVA, T., KURKIN, A., KOZELKOV, A., and ZAITSEV, A.(2004). *Tsunamis in the Black Sea: comparison of the historical, instrumental, and numerical data*. J. Geophys. Res., *109*, C12023.

YALCINER, A.C., and PELINOVSKY, E.F. (2007). *A short cut numerical method for determination of periods of free oscillations for basins with irregular geometry and bathymetry*, Ocean Eng., *34*, 5-6, 747–757.

YAO, L.S. (1999). *A resonant wave theory*. J. Fluid Mechanics, *395*, 237-251.

YANUMA, T., and TSUJI, Y. (1998). *Observation of edge waves trapped on the continental shelf in the vicinity of Makurazaki Harbor, Kyushu, Japan*. J. Oceanography, *54*, 1, 9-18.

ZELT, J.A., and RAICHLEN, F. (1990). *A Lagrangian model for wave-induced harbour oscillations*. J. Fluid Mechanics, *213*, 1, 203-225.